

# Fractality of eroded coastlines of correlated landscapes

P. A. Morais,<sup>1,\*</sup> E. A. Oliveira,<sup>1,†</sup> N. A. M. Araújo,<sup>2,‡</sup> H. J. Herrmann,<sup>1,2,§</sup> and J. S. Andrade Jr.,<sup>1,¶</sup>

<sup>1</sup>*Departamento de Física, Universidade Federal do Ceará, 60451-970 Fortaleza, Ceará, Brazil*

<sup>2</sup>*Computational Physics for Engineering Materials, IfB,  
ETH Zürich, Schafmattstr. 6, 8093 Zürich, Switzerland*

We investigate through numerical simulations of a simple sea-coast mechanical erosion model, the effect of spatial long-range correlations in the lithology of coastal landscapes on the fractal behavior of the corresponding coastlines. In the model, the resistance of a coast section to erosion depends on the local lithology configuration as well as on the number of neighboring sea sides. For weak sea forces, the sea is trapped by the coastline and the eroding process stops after some time. For strong sea forces erosion is perpetual. The transition between these two regimes takes place at a critical sea force, characterized by a fractal coastline front. For uncorrelated landscapes, we obtain, at the critical value, a fractal dimension  $D = 1.33$ , which is consistent with the dimension of the accessible external perimeter of the spanning cluster in two-dimensional percolation. For sea forces above the critical value, our results indicate that the coastline is self-affine and belongs to the KPZ universality class. In the case of landscapes generated with power-law spatial long-range correlations, the coastline fractal dimension changes continuously with the Hurst exponent  $H$ , decreasing from  $D = 1.34$  to  $1.04$ , for  $H = 0$  and  $1$ , respectively. This non-universal behavior is compatible with the multitude of fractal dimensions found for real coastlines.

PACS numbers: 89.75.Da, 92.40.Gc, 64.60.al, 64.60.ah

## I. INTRODUCTION

Since the introduction of the concept of fractals by Mandelbrot [1], scale invariant behavior has been identified and investigated in many geological and geophysical phenomena [2], including the frequency distributions of earthquakes [3] and volcanic eruptions [4], the size distribution of rock fragments [5, 6] and mineral deposits [7], and the topography of river networks [8, 9], rivers deltas [10] and rocky coastlines [11, 12]. More recently, the geometry of watersheds, namely, the lines separating adjacent drainage basins (catchments), has been reported to display also typical fractal features [13–15], with important implications to water management [16], landslides [17, 18], and flood prevention [19].

Erosion is certainly one of the most remarkable examples of a geological process that naturally generates diverse self-similar structures. In particular, the erosion of a coastline by the sea [20] constitutes a rather rich phenomenon. Due to the action of underlying geological processes (e.g., tectonics and volcanic events), topological and lithological properties of coastal landscapes are generally heterogeneous as well as long-range correlated in space. As a consequence, the resistance to erosion must be considered as a spatially dependent parameter. One should therefore expect that the self-similar geometry of coastlines should emerge from an intricate interplay between these landscape properties and the sea force.

In a study by Sapoval *et al.* [21], an erosion model is proposed to show how surviving coastlines can dynamically evolve to self-similar objects by means of a self-organized critical process [22, 23]. By applying this model to spatially uncorrelated landscapes, they recovered, at the critical steady-state, a fractal dimension  $D = 1.33$  that is frequently observed in real systems [12]. This dimension is different from  $7/4$ , the dimension of the external perimeter of percolation [24], but it is consistent with  $4/3$ , the one for the accessible external perimeter [25]. This value, however, cannot be taken as universal, since, in fact, a multitude of fractal dimensions has been measured for real coastlines [26].

In this work, we investigate the dependence of the fractal dimension of sea-coast interfaces on the long-range correlations of synthetic landscapes. In order to study the invasion of the sea through the coast we consider a simple lattice invasion model. Each coast site is characterized by a resistance to erosion which is a function of its local lithology parameter and coastal configuration. Spatial long-range correlated surfaces are generated with the Fourier filtering method [27–31], which allows to control the nature and the strength of correlations.

The manuscript is organized as follows. In Section II we introduce the model and its relevant definitions. Results for correlated and uncorrelated distributions of the lithology are discussed in Section III. Finally, conclusions are drawn in Section IV.

## II. THE MODEL

In a recent work, Sapoval *et al.* [21] proposed a model that explicitly split the dynamics of erosion into two different mechanisms based on their characteristic time scale,

\* pablo@fisica.ufc.br

† erneson@fisica.ufc.br

‡ nuno@ethz.ch

§ hans@ifb.baug.ethz.ch

¶ soares@fisica.ufc.br

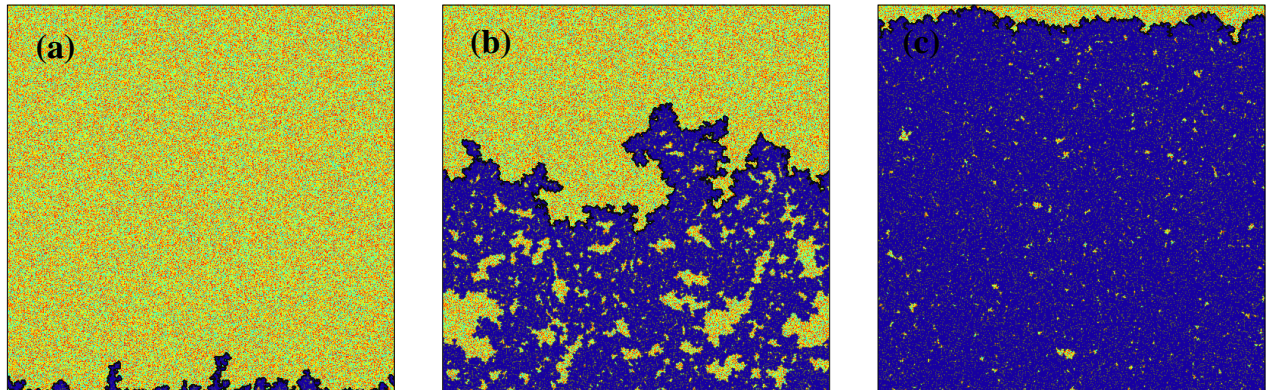


FIG. 1. (color online) Snapshots of typical configurations obtained with the erosion model for uncorrelated lithology on a lattice with  $512^2$  sites. The sea sites are in blue (dark grey) and all the other sites are land sites (light grey). Three different regimes are obtained: a) subcritical, weak sea force, regime ( $f < f_c$ ): the coastline is rough but not fractal. b) critical regime ( $f = f_c$ ): the coastline is a self-similar fractal. c) supercritical, strong sea force, regime ( $f > f_c$ ): the coastline is no longer self-similar, but rather self-affine.

namely, slow and rapid dynamics. While the former is mainly related to chemical processes, the latter is solely due to mechanical erosion. Here we only focus on the rapid dynamics, since the slow one takes place on a time scale which is beyond the scope of this study.

For simplicity, the system is mapped onto a regular square lattice, where each site can be either a sea or a land site. For land coast site, a lithology param-

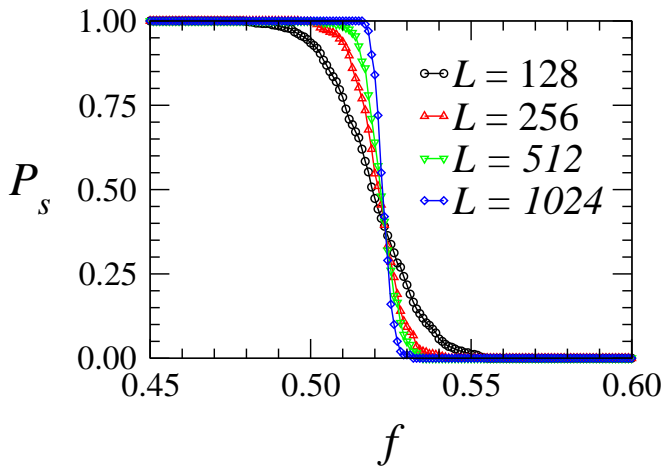


FIG. 2. (color online) Dependence of the sea-trapping probability,  $P_s$ , on the erosion force  $f$ , for landscapes generated with a uniform distribution of the lithology parameter  $\ell$ . A transition is observed from a trapped, subcritical, regime – for weak sea force – to a perpetual, supercritical, invasion regime – for strong sea force. The transition occurs for  $f_c = 0.523 \pm 0.001$  – estimated from the crossing of the lines. Each curve corresponds to a different system size  $L^2$ , with  $L = \{128, 256, 512, 1024\}$ , and results have been averaged over  $\{800, 400, 200, 100\}$  samples, respectively.

ter  $\ell_i$  is assigned, which coarse-grains several geological properties, characterizing the mechanical interaction with the sea. We assume that an island site completely

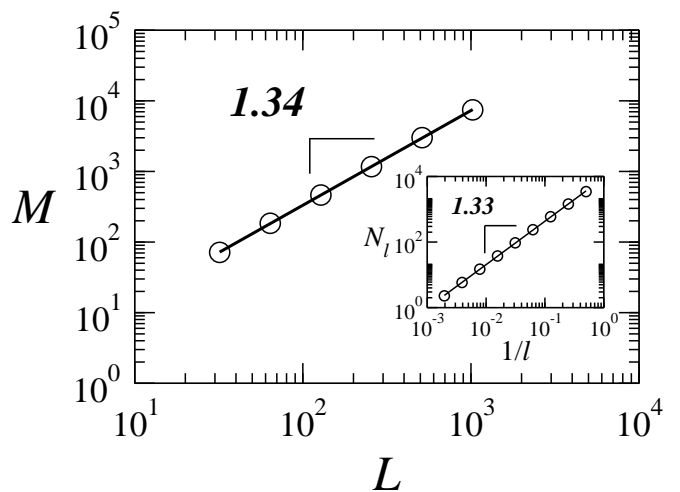


FIG. 3. Size dependence of the mass of the coastline – number of sites – at the critical sea force,  $f = f_c$ . A fractal dimension  $D = 1.34 \pm 0.01$  is obtained from the best fit of the data points. Square lattices, with uniform distribution of the lithology parameter, of size  $L^2$  have been considered with  $L = \{32, 64, 128, 256, 512, 1024\}$ . Results have been averaged over  $\{3200, 1600, 800, 400, 200, 100\}$  independent realizations. The inset shows, for the yardstick method, the number of sticks needed to cover the line as a function of the inverse of the stick size, for a system with  $L = 1024$ , averaged over  $10^2$  samples. From the fit, a fractal dimension  $D = 1.33 \pm 0.01$  is obtained. From both methods the fractal dimension of the coastline in the critical regime is estimated to be  $D = 1.33 \pm 0.01$ .

surrounded by the sea is more fragile than a similar one in the coastline, so that the resistance to erosion  $r_i$  depends on the local coastal configuration as,

$$r_i = \ell_i^{n_i}, \quad (1)$$

where  $n_i$  is the number of neighboring sea sites. Accordingly, a coast site with only one sea neighbor has resistance  $r_i = \ell_i$ , while one completely clipped by water has resistance  $r_i = \ell_i^4$ . During the invasion process, the sea penetrates in the coastline with a constant force  $f$ . Initially, the coastline, defined as the interface between sea and land, is a straight line at the bottom of the system and periodic boundary conditions are applied in the horizontal direction. At each iteration, all coast sites in the neighborhood of a sea site, and with a resistance to erosion below the sea force, become part of the sea. The proposed model corresponds to a collective invasion percolation where the resistance is a function of the number of neighboring sea sites. For  $r_i = \ell_i$  the resistance is solely dependent on the lithology parameter and ordinary percolation is recovered. The introduced weakening mechanism promotes the erosion of earth filaments in the coast, typically observed for ordinary percolation.

### III. RESULTS

#### A. Uncorrelated lithology

Let us start with the study of the model on an uncorrelated lithology, where the lithology parameter is uniformly distributed in the range  $0 < \ell < 1$ . Figure 1 shows a typical configuration of the system for different sea forces  $f$  and obtained for the same distribution of the lithology parameter. Two different regimes are observed based on the sea force, namely, a weak and a strong regime. For weak sea force, as shown in Fig. 1(a), corresponding to low values of  $f$ , only few sites are eroded and invaded by the sea. After some finite number of steps, the sea is completely trapped by the coastline – the resistance of all coastline sites is greater than the sea force – and the sea cannot invade further. For strong sea force, Fig. 1(c), the coastline perpetually grows, without being ever trapped. Nevertheless, some islands remain that will never be destroyed, i.e., their coastline sites have a resistance above the sea force. As discussed before, in reality two different mechanisms occur: the mechanical and the chemical erosion. In this work, we solely account for the former one, however, over larger time scales, due to the latter mechanism the sea is permanently eroding the coastline.

The transition between the weak and the strong sea force regimes occurs at a critical force  $f = f_c$ . To determine this critical force, we analyze the sea-trapping probability defined as the probability, for a given sea force, for an erosion process to be limited to a finite number of iterations. In Fig. 2 we show this probability as a function of the sea force, for different system sizes. For the weak sea

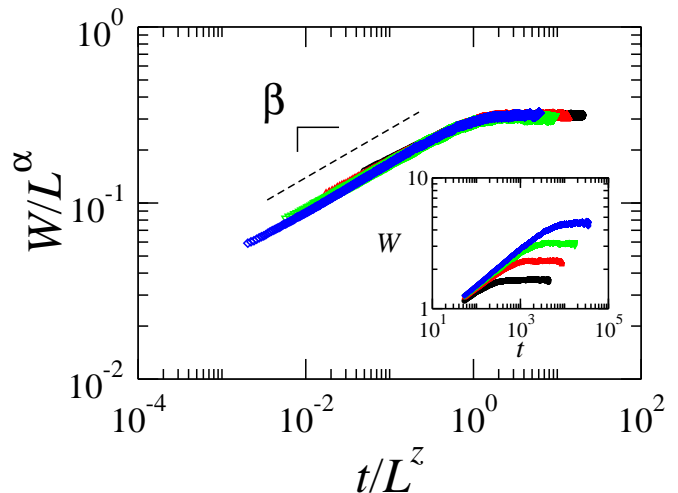


FIG. 4. (color online) Finite-size scaling of the time dependence of the coastline roughness in the supercritical regime ( $f = 0.9$ ). Square lattices with  $L_x \times L_y$  sites have been considered, with  $L_x = L$  and  $L_y = 128L$ . The time  $t$  has been rescaled by  $L^z$ , where  $z$  is the dynamic exponent, and the roughness has been rescaled in units of  $L^\alpha$ , where  $\alpha$  is the roughness exponent. The best data collapse is obtained for  $\alpha = 0.48 \pm 0.04$  and  $z = 1.55 \pm 0.11$ , a value that is consistent with the Kardar-Parisi-Zhang universality class [32]. The straight line has slope  $\beta$ , corresponding to the growth exponent. The inset shows the time dependence of the coastline roughness. Systems with  $L = \{32, 64, 128, 256\}$  have been sampled over  $\{3200, 1600, 800, 400\}$  independent runs, respectively.

force,  $f < f_c$ , since the sea invasion is always halted after some steps, the probability is one. On the other hand, in the strong sea force regime,  $f > f_c$ , the sea erosion is never stopped. From the crossing of all lines (different system sizes), it is possible to estimate the critical force as  $f_c = 0.523 \pm 0.001$ . At the critical force, the front of the coastline is self-similar with a fractal dimension  $D = 1.33 \pm 0.01$ . To obtain the fractal dimension, we considered two different methods: the scaling of the set of coastal sites with system size (main plot of Fig. 3) and the yardstick method (inset of Fig. 3) [33]. The critical force obtained under the proposed weakening mechanism is lower than the one corresponding to ordinary percolation ( $f_c \approx 0.593$ ), recovered when the resistance is solely dependent on the lithology parameter, in the absence of weakening. In such case, the obtained fractal dimension is compatible with  $7/4$ , the one of the hull of the percolation cluster [25].

For strong sea force,  $f > f_c$ , the sea constantly erodes the coast, being never trapped, and the resulting coastline front is self-affine. Moreover, our results indicate that the statistical properties of the sea invasion process belong to the same universality class of interfaces that obey the Kardar-Parisi-Zhang (KPZ) equation [32]. To characterize the main interface (coastline front), we study the time evolution of the roughness,  $W$ , namely,

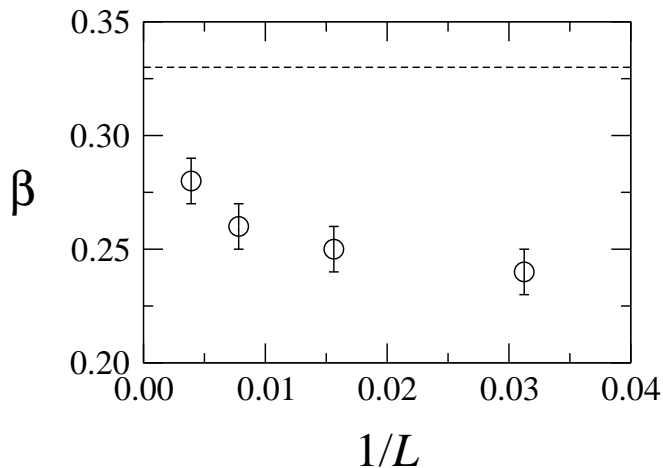


FIG. 5. Size dependence of the growth exponent,  $\beta$ . These results indicate that, in the thermodynamic limit,  $\beta$  converges to  $\beta = 1/3$  (dashed line) as in the Kardar-Parisi-Zhang universality class. Systems with  $L = \{32, 64, 128, 256\}$  have been sampled over  $\{3200, 1600, 800, 400\}$  independent runs, respectively.

the standard deviation of the interface width, defined as,

$$W = \sqrt{\frac{1}{L} \sum_{i=1}^L (y_i - \langle y \rangle)^2}, \quad (2)$$

where  $y_i$  is the vertical position of the interface and  $\langle y \rangle$  its mean value over all columns. Results for different system sizes are shown in the inset of Fig. 4. Initially, the roughness is an algebraic function of time,  $W \sim t^\beta$ , where  $\beta$  is the growth exponent. At a certain crossover,  $t = t_\times$ , lateral correlations in space resulting from the invasion process become so large, as compared to the finite size  $L$ , that the roughness reaches a saturation value,  $W_{\text{sat}}$  [34]. With the system size,  $W_{\text{sat}}$  diverges as  $W_{\text{sat}} \sim L^\alpha$  and the crossover time scales as  $t_\times \sim L^z$ , where  $\alpha$  is the roughness exponent and  $z$  the dynamic exponent. Therefore, a complete finite-size scaling can be obtained with the *ansatz* [35],

$$W(L, t) = L^\alpha \left( \frac{t}{L^z} \right). \quad (3)$$

The main plot of Fig. 4 corresponds to the finite-size scaling of the roughness. From the data collapse, we obtain the values  $\alpha = 0.48 \pm 0.04$  and  $z = 1.55 \pm 0.11$ , which are consistent with the exponents  $\alpha = 1/2$  and  $z = 3/2$  from the KPZ universality class [32, 36]. The size dependence of the growth exponent is shown in Fig. 5. Our results indicate that, in the thermodynamic limit, the growth exponent converges to the expected KPZ value of  $\beta = 1/3$ . For strong sea force, when the weakening by neighboring sea sites is neglected, the supercritical regime of ordinary percolation is recovered.

## B. Correlated lithology

In this section we discuss the case where the disordered coastal landscapes possess spatial long-range correlations in the lithology parameter  $\ell$ . As in previous studies [28–31, 37–43], spatial long-range correlated distributions are obtained with fractional Brownian motion (fBm) [1, 27]. To achieve the intended correlated distribution, Fourier coefficients are generated in the reciprocal space of frequencies  $f$ , according to a power-law spectral density, namely,

$$S(f_1, \dots, f_d) = \left( \sqrt{\sum_{i=1}^d f_i^2} \right)^{-w}, \quad (4)$$

where  $d$  is the spatial dimension ( $d = 2$  in this work), and the inverse Fourier transform is applied to obtain the distribution in real space. Several samples are then generated and the distributions truncated between  $-3\sigma$  and  $3\sigma$ , where  $\sigma$  is the standard deviation. The truncation is such that values outside this range are assigned to be  $\pm 3\sigma$ , keeping the original sign. Finally, the distribution is rescaled in the interval  $[0:1]$ . Each distribution is characterized by a Hurst exponent  $H$  – related to the spectral exponent by  $w = 2H + d$  – such that, for two dimensions, the correlations are negative for  $0 < H < 1/2$  and positive for  $1/2 < H < 1$ . The former case means that neighbors of a strong site are, on average, weak sites, whereas in the latter case they are typically strong sites. For  $H = 1/2$ , the classical Brownian motion is recovered where the increments are uncorrelated but the obtained lithology is still correlated. The uncorrelated distribution of lithology is solely obtained for a constant spectral density, with  $w = 0$  and  $H = -d/2$  ( $H = -1$  in two dimensions). Further details about the adopted methodology can be found, for example, in Ref. [31].

Figure 6 shows snapshots of the system, at the critical force, for three different values of the Hurst exponent, namely, 0, 0.2, and 0.8. In the first two the spatial correlations are negative, while the latter corresponds to a strong positive correlation. By increasing the Hurst exponent, islands become less frequent and the interface smooths out. In the limit of very strong positive correlations, the coastline converges to a non-fractal object with dimension one. In Fig. 7 we show the fractal dimension of the coastline front  $D$  as a function of the Hurst exponent. The fractal dimension decreases continuously from  $D = 1.34 \pm 0.02$ , for  $H = 0$ , to  $D = 1.04 \pm 0.03$ , for strong positive correlations.

## IV. CONCLUSIONS

In this work, a model is introduced to study the mechanical erosion of the coastline by the sea. Despite sharing some features with invasion percolation, in this model the update occurs over the entire interface and not only

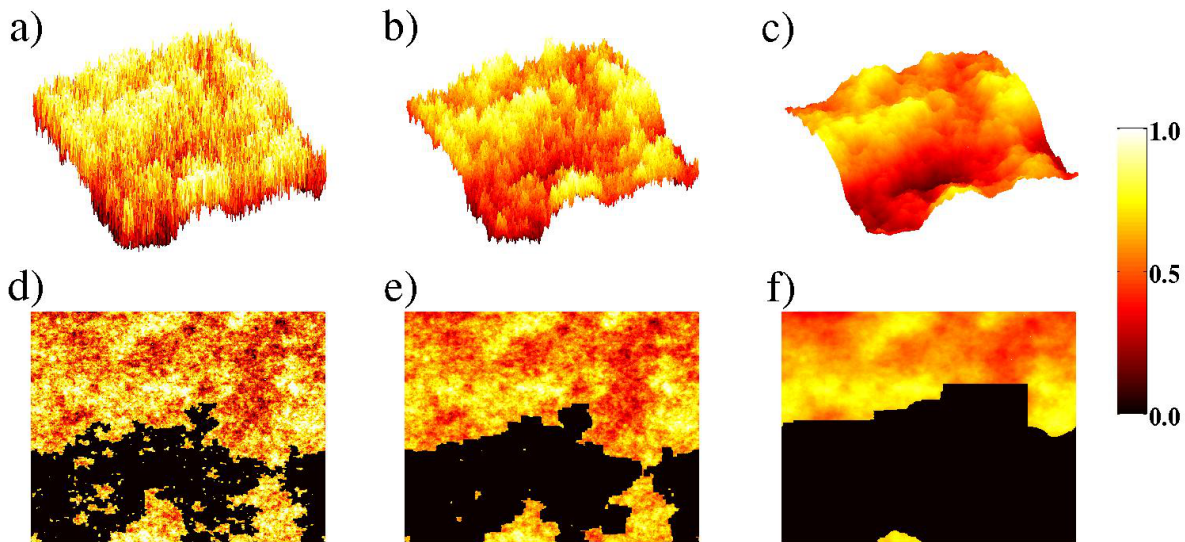


FIG. 6. (color online) Snapshots of the initial distribution of lithology parameter (a, b, and c) and the corresponding eroded system (d, e, and f) at the critical force ( $f = f_c$ ), for three landscapes generated with long-range spatial correlations, for different Hurst exponent: a) and d)  $H = 0.0$ ; b) and e)  $H = 0.2$ ; and c) and f)  $H = 0.8$ . The color scheme of coast sites represents the value of the lithology parameter  $l$  and sea sites were assigned with  $l = 0$ . Pictures have been obtained for square lattices with  $512^2$  sites.

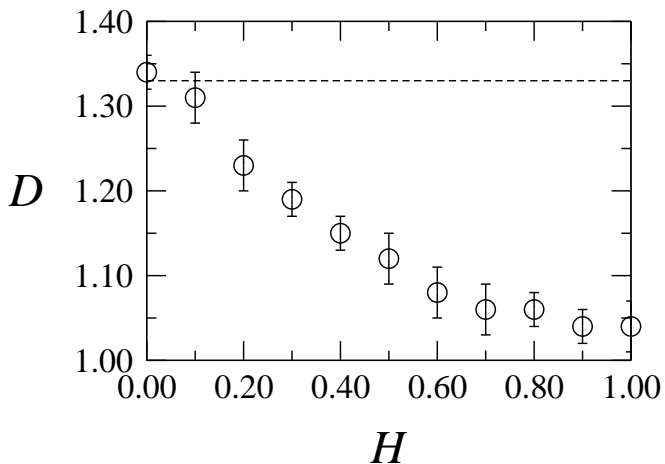


FIG. 7. Critical coastline fractal dimension  $D$  as a function of the Hurst exponent  $H$ . A continuous decrease from  $D = 1.34$  at  $H = 0$  to  $D = 1.04$  at  $H = 1.0$  is observed. The dashed line stands for the fractal dimension of the uncorrelated case ( $D = 1.33$ ). Each point is obtained from the size dependence of the number of coastline sites for system sizes  $L = \{32, 64, 128, 256, 512, 1024\}$  averaged over  $\{3200, 1600, 800, 400, 200, 100\}$  samples.

at a single interface site and the resistance of a coast site to erosion depends on the local configuration. The larger the number of neighboring sea sites the weaker the resistance. We have shown that, based on the sea force, the system can either be in the weak or strong sea force regime. While in the former the sea is trapped by

the coastline and the eroding process stops after some time, in the latter, erosion is perpetual and belongs to the Kardar-Parisi-Zhang universality class. The transition between these two regimes occurs at a critical sea force, characterized by a fractal coastline front. For an uncorrelated distribution of the coast lithological properties, the fractal dimension of this interface is related with the accessible perimeter of the percolation cluster, whereas for coasts with long-range correlation, the fractal dimension changes with the Hurst exponent. In Ref. [21] a model with a self-stabilization mechanism is proposed to explain how the system is found at criticality. Here, we solely focus on the effect of correlations on the properties of the critical state without self-organization. Yet, this study clarifies the relation between the spatial correlations in the lithology and the multitude of fractal dimensions observed for coastlines. As an extension of this work, one might consider the effect of disorder in the strong sea force regime.

## ACKNOWLEDGMENTS

We thank Bernard Sapoval and Andrea Baldassarri for fruitful discussions. We also thank the ETH Competence Center Coping with Crises in Complex Socio-Economic Systems (CCSS) through the ETH Research Grant CH1-01-08-2, the Brazilian agencies CNPq, CAPES and FUNCAP, and the Pronex grant CNPq/FUNCAP, for financial support.

- 
- [1] B. B. Mandelbrot, *Science*, **156**, 636 (1967).
- [2] D. L. Turcotte, *Pure Appl. Geophys.*, **131**, 171 (1989).
- [3] D. Sornette, *Phys. Rev. Lett.*, **72**, 2306 (1994); A. Saichev and D. Sornette, *ibid.*, **97**, 078501 (2006); E. Lippiello, C. Godano, and L. de Arcangelis, *ibid.*, **98**, 098501 (2007); M. Bottiglieri, L. de Arcangelis, C. Godano, and E. Lippiello, *ibid.*, **104**, 158501 (2010).
- [4] E. Kaminski and C. Jaupart, *J. Geophys. Res.*, **103**, 29759 (1998).
- [5] J. A. Aström, *Adv. Phys.*, **55**, 247 (2006).
- [6] F. Kun, F. K. Wittel, H. J. Herrmann, B. H. Kröplin, and K. J. Maløy, *Phys. Rev. Lett.*, **96**, 025504 (2006).
- [7] Z. R. Zhang, H. H. Mao, and Q. M. Cheng, *Math. Geol.*, **33**, 217 (2001).
- [8] J. R. Banavar, A. Maritan, and A. Rinaldo, *Nature*, **399**, 130 (1999).
- [9] P. S. Dodds, *Phys. Rev. Lett.*, **104**, 048702 (2010).
- [10] H. Seybold, J. S. Andrade Jr., and H. J. Herrmann, *P. Natl. Acad. Sci. USA*, **104**, 16804 (2007); H. J. Seybold, P. Molnar, D. Akca, M. Doumi, M. C. Tavares, T. Shinbrot, J. S. Andrade, W. Kinzelbach, and H. J. Herrmann, *Geophys. Res. Lett.*, **37**, L08402 (2010).
- [11] A. Baldassarri, M. Montuori, O. Prieto-Ballesteros, and S. C. Manrubia, *J. Geophys. Res.*, **113**, E09002 (2008).
- [12] G. Boffetta, A. Celani, D. Dezzani, and A. Seminara, *Geophys. Res. Lett.*, **35**, L03615 (2008).
- [13] E. Fehr, J. S. Andrade Jr., S. D. da Cunha, L. R. da Silva, H. J. Herrmann, D. Kadau, C. F. Moukarzel, and E. A. Oliveira, *J. Stat. Mech.*, P09007 (2009).
- [14] E. Fehr, D. Kadau, J. S. Andrade Jr., and H. J. Herrmann, *Phys. Rev. Lett.*, **106**, 048501 (2011).
- [15] J. S. Andrade Jr., S. D. S. Reis, E. A. Oliveira, E. Fehr, and H. J. Herrmann, *Comput. Sci. Eng.*, **13**, 74 (2010).
- [16] C. J. Vorosmarty, C. A. Federer, and A. L. Schloss, *J. Hydrol.*, **207**, 147 (1998); A. Y. Kwarteng, M. N. Viswanathan, M. N. Al-Senafy, and T. Rashid, *J. Arid. Environ.*, **46**, 137 (2000); A. Sarangi and A. K. Bhat-tacharya, *Agric. Water Manage.*, **78**, 195 (2005).
- [17] A. S. Dhakal and R. C. Sidle, *Hydrol. Processes*, **18**, 757 (2004); B. Pradhan, R. P. Singh, and M. F. Buchroithner, *Adv. Space Res.*, **37**, 698 (2006); M. Laz-zari, E. Gerdali, V. Lapenna, and A. Loperte, *Land-slides*, **3**, 275 (2006).
- [18] K. T. Lee and Y. T. Lin, *J. Am. Water Resour. Assoc.*, **42**, 1615 (2006).
- [19] P. Burlando, M. Mancini, and R. Rosso, *IFIP Trans. B*, **16**, 91 (1994); D. Q. Yang, Y. Zhao, R. Armstrong, D. Robinson, and M. Brodzik, *J. Geophys. Res. Earth Surf.*, **112**, F02S22 (2007).
- [20] E. C. Penning-Roswell, C. H. Green, P. M. Thompson, A. M. Coker, S. M. Tunstall, C. Richards, and D. J. Parker, *The Economics of Coastal Management* (Bel-haven Press, London, 1992).
- [21] B. Sapoval, A. Baldassarri, and A. Gabrielli, *Phys. Rev. Lett.*, **93**, 098501 (2004).
- [22] P. Bak, *How nature works? The science of self-organized criticality* (Springer-Verlag New York, United States of America, 1996).
- [23] D. L. Turcotte, *Rep. Prog. Phys.*, **62**, 1377 (1999).
- [24] B. Sapoval, M. Rosso, and J. F. Gouyet, *J. Physique Lett.*, **46**, L149 (1985).
- [25] T. Grossman and A. Aharony, *J. Phys. A*, **20**, L1193 (1987).
- [26] L. F. Richardson, *Gen. Syst. Yearb.*, **6**, 139 (1961).
- [27] H. Peitgen and D. Saupe, eds., *The Science of Fractal Images* (Springer, New York, 1988).
- [28] M. Sahimi, *J. Phys. I France*, **4**, 1263 (1994).
- [29] M. Sahimi and S. Mukhopadhyay, *Phys. Rev. E*, **54**, 3870 (1996).
- [30] H. A. Makse, S. Havlin, M. Schwartz, and H. E. Stanley, *Phys. Rev. E*, **53**, 5445 (1996).
- [31] E. A. Oliveira, K. J. Schrenk, N. A. M. Araújo, H. J. Herrmann, and J. S. Andrade Jr., *Phys. Rev. E*, **83**, 046113 (2011).
- [32] M. Kardar, G. Parisi, and Y. C. Zhang, *Phys. Rev. Lett.*, **56**, 889 (1986).
- [33] C. Tricot, J. F. Quiniou, D. Wehbi, C. Roquesarmes, and B. Dubuc, *Revue Phys. Appl.*, **23**, 111 (1988).
- [34] A.-L. Barabási and H. E. Stanley, *Fractal Concepts in Surface Growth* (Cambridge University Press, United Kingdom, 1995).
- [35] F. Family and T. Vicsek, *J. Phys. A*, **18**, L75 (1985).
- [36] G. Ódor, *Rev. Mod. Phys.*, **76**, 663 (2004).
- [37] S. Prakash, S. Havlin, M. Schwartz, and H. E. Stanley, *Phys. Rev. A*, **46**, R1724 (1992).
- [38] E. S. Kikkinides and V. N. Burganos, *Phys. Rev. E*, **59**, 7185 (1999).
- [39] H. E. Stanley, J. S. Andrade Jr., S. Havlin, H. A. Makse, and B. Suki, *Physica A*, **266**, 5 (1999).
- [40] H. A. Makse, J. S. Andrade Jr., and H. E. Stanley, *Phys. Rev. E*, **61**, 583 (2000).
- [41] A. D. Araújo, A. A. Moreira, H. A. Makse, H. E. Stanley, and J. S. Andrade Jr., *Phys. Rev. E*, **66**, 046304 (2002).
- [42] A. D. Araújo, A. A. Moreira, R. N. Costa Filho, and J. S. Andrade Jr., *Phys. Rev. E*, **67**, 027102 (2003).
- [43] C. Du, C. Satik, and Y. C. Yortsos, *AIChE Journal*, **42**, 2392 (1996).